OPEN GEOMECHANICS

Removal of the membrane penetration error from triaxial data

Andrzej Niemunis [a] ***& Lukas Knittel*** [a]

[a] *Karlsruhe Institute of Technology (KIT), Institute of Soil Mechanics and Rock Mechanics (IBF).*

Published
9th December 2020
https://doi.org/10.5802/ogeo.7

Edited by
Jelke Dijkstra
Chalmers University of Technology, Gothenburg, Sweden

Reviewed by
Three anonymous reviewers

Correspondence
Andrzej Niemunis
Karlsruhe Institute of Technology (KIT), Institute of Soil Mechanics and Rock Mechanics (IBF) Engler-Bunte-Ring 14, 76131 Karlsruhe
Germany
andrzej.niemunis@kit.edu

Open Geomechanics is member of the Centre Mersenne for Open Scientific Publishing

Abstract. Most triaxial tests are fraught with substantial membrane penetration errors. A simple correction procedure for data obtained from various tests is proposed. Correction formulas for the membrane penetration error have been derived for different types of tests including not perfectly saturated soils. In particular, a correction of the undrained cyclic stress paths is presented in detail. It is demonstrated that the correction for the membrane penetration error is indispensable for a realistic estimation of the cyclic resistance ratio in coarse- and medium-grained liquefiable soils. A MATHEMATICA code for the correction of laboratory data is given. An analogous MATLAB code is available from the authors. Without the correction many results could lie far on the unsafe side. This is the case especially for the undrained cyclic loading.

Keywords. Membrane penetration, triaxial test, cyclic loading, CRR, Mathematica

1. Introduction

In triaxial tests, the isochoric (constant-volume) conditions are approximated by imposing undrained conditions (closing the pore-water valve) and by keeping the sample perfectly saturated. A discrepancy between the undrained and isochoric conditions is caused by the so-called membrane penetration (MP) and by the compressibility of the substance. This problem is the main subject of the presented paper.

In the opencast lignite mines like Hambach (Germany), see Fig.1, the loosely dumped granular layers may reach the depth of 400 m. For the re-cultivation of the region, the stability of such layers after ground-water flooding is of great interest. According to the local seismic data, small to moderate earthquakes may be expected in the region. They may lead to spontaneous liquefaction of loose soil deposits and to catastrophic events known as *settlement flow* (ger. "Setzungsfließen"), especially from East Germany. Hence, the resistance to liquefaction should be well evaluated.

For reliable predictions of cyclic stability of loose deposits and their slopes, undrained cyclic triaxial tests are necessary. A parameter commonly used is the cyclic resistance ratio (CRR) after Vaid et al. [1990]

$$\mathrm{CRR}(N_f = 10) = \frac{1}{2} q^{\mathrm{ampl}} / p_0 \tag{1}$$

If $N_f = 10$ undrained triaxial cycles with the stress amplitude q^{ampl} are applied starting from the isotropic effective pressure p_0, then a liquefaction is expected. Of course, CRR may depend not only on a type of soil but also on the density and some more subtle parameters of soil structure, aging etc. Due to the influence of the MP, the experimental evaluation of the CRR needs to be critically revised. In this context, the MP has numerous literature Ansal and Erken [1996], Frydman et al. [1973], Haeri and Shakeri [2010], Kiekbusch and Schuppener [1977], Newland and Alley [1957], Raju and Sadasivian [1974], Raju and Venkatramana [1980], Ramana and Raju [1982], Roscoe et al. [1963], Seed et al. [1989], Tokimatsu and Nakamura [1986], Vaid and Negussey [1984], Wichtmann [2005], Wichtmann et al. [2019].

Unfortunately, most authors deal with empirical formulas for the MP. They are based on fragmentary data and can hardly be considered as proven in the sense of statistics. Correlations of the MP with the grain size distribution alone and without asperity seem disputable. Only few authors Ramana and Raju [1982], Tokimatsu [1990], Wichtmann et al. [2019] deal with the accumulation of the MP during cyclic tests. The proposed overall MP-factors can be applied to the end results only. To the best knowledge of the authors, no incremental procedure to eliminate the MP-effect from the measured paths has been proposed as yet. This article tries to fill this gap providing a general approach to the MP based on the incrementally linear constitutive formalism. Nevertheless the empirical formulas can still enter the calculation via the parameter k_{MP}, see Eq. (2).

During evaluation of the CRR, a difference between undrained and isochoric conditions due to the MP may be of importance as demonstrated in Section 5. For fine materials, the influence of the MP is negligible but for coarse-grained materials it is essential to purify the data from the MP-errors. The MP is known for affecting the triaxial data for soils with $d_{20} > 1$ mm. However, also for medium-grained sand the MP-errors can be quite considerable as demonstrated in Section 5.

Grains penetrate into the membrane and this spoils the accuracy of the volumetric deformation, if measured via the pore water system. Another effect of the MP is the discrepancy between undrained and isochoric condition. Undrained and isochoric stress paths may strongly differ despite perfect saturation of the sample. The isochoric conditions may be also spoiled by the compressibility of the pore fluid due to poor saturation. Poor saturation can be easily detected via the Skempton parameter $B = \dot{u}/\dot{p}^{\mathrm{tot}}$ being smaller than unity, Skempton [1954]. Unfortunately, the diagnosis of the MP effect is more complicated. Figure 2 presents the CRR of the Karlsruhe sand from samples of different size. The influence of the diameter of the sample is evident. Different ratios of the surface of the membrane to the volume of the sample cause different MP errors and hence different CRRs. Evidently, the membrane penetration affects the CRR values. This will be examined in the context of liquefaction of deposited soils.

1.1. Notation

Geotechnical sign convention and homogeneous stress and strain fields are assumed. The usual triaxial symmetries hold. Roscoe invariants for strains and stresses (work conjugated) are used. The corresponding stiffness is written as a 2×2 matrix. The superposed dot $\dot{\square}$ denotes a small increment of $\square$. Effective stress is written without dash throughout the text. A consistent system of units should be used with [m], [kN], [kPa], [s] except for the empirical formulas wherein the units are specified.

Essential variables:

$\dot{\varepsilon}_a, \dot{\varepsilon}_r$ = axial and radial strain rate components
$\dot{\varepsilon}_{\mathrm{vol}} = \dot{\varepsilon}_a + 2\dot{\varepsilon}_r,\ \dot{\varepsilon}_q = \frac{2}{3}(\dot{\varepsilon}_a - \dot{\varepsilon}_r)$ Roscoe strain rates
σ_a, σ_r = axial and radial stress components
$p = (\sigma_a + 2\sigma_r)/3,\ q = \sigma_a - \sigma_r$ Roscoe stress invariants
V_w, V = water volume and volume of the triaxial sample
u = pore water pressure and air pressure in the bubbles
$\square^{\mathrm{tot}} = \square + u$ total stress component
K, G = bulk modulus, shear modulus
K_{pq}, K_{qp} = coupling terms
$\square^*$ = value of $\square$ blurred by the MP
$h, h_0 = \dot{p}/\dot{q}$ inclinations of stress increment
$\square^{MP}$ = $\square$ due to MP
$\square^{\mathrm{ampl}}$ = amplitude of $\square$
K_a, K_w, K_s, K_m = bulk modulus of the substance (air, water, quarz, mixture)
$M_e = q_{\max}/p$ inclination of the tx. extension failure line
N_f number of cycles to failure
n = porosity
k_{MP} = proportionality factor from Eq. (2)
n_K, n_k = exponents for $K \sim p^{n_K}$ and $k_{MP} \sim p^{n_k}$
S_r = degree of saturation
S^{MP} = a membrane parameter after Nicholson et al. [1993]

Figure 1. *View of the extraction side of the lignite opencast mine Hambach (on the left-hand side) with a surface of 85 km^2 and depth 400 m created with coal excavator and dumping site (right hand side) in October 2018*

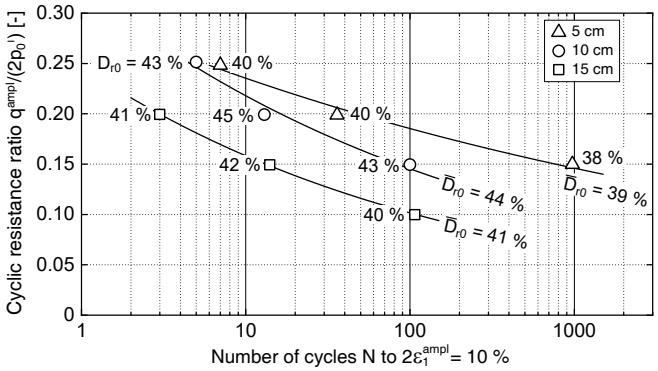

Figure 2. *CRR as a function of the number of cycles N to failure ($2\varepsilon^{ampl}$ = 10 %). Karlsruhe Sand with relative density $D_{r0} \approx 0.4$ but different sizes (diameter = height).*

Z, p_Z = parameters of stiffness by Osinov et al. [2016]
h_B, n_B = parameters of compression curve by Bauer [1992]
A_{mem} = surface of the membrane
A_S, A = original and modified parameter by Skempton [1954]

2. Volumetric strain measured via the pore water system

The MP is caused by changes in the effective radial stress $\dot\sigma_r$, Fig. 3a. In drained tests, the MP affects the volume of pore water squeezed out from the sample and hence $\dot\varepsilon_{\mathrm{vol}} \approx \Delta V_w/V$ is not exactly equal to the volumetric deformation of the soil skeleton. The undrained strength can be deceitfully large compared to the true isochoric value c_u of loose samples, Fig. 3b. As a portion of the volumetric strain rate, the MP-error can be assumed proportional to the radial stress rate

$$\dot\varepsilon_{\mathrm{vol}}^{MP} = \dot\sigma_r / k_{MP}\,, \tag{2}$$

wherein the factor k_{MP} may be treated as a constant within a single increment. Sophisticated stress functions are being used to quantify the MP. An additional radial compression due to the tension in the membrane is neglected[(1)] here.

In this work, a perfectly saturated triaxial sample, $S_r = 1$ with incompressible substance

$$K_m = [n(1-S_r)/K_a + nS_r/K_w + (1-n)/K_s]^{-1} = [n/K_w + (1-n)/K_s]^{-1} \approx \infty \tag{3}$$

is assumed everywhere except Sections 4.3 and 4.4. Let the sample be tested under perfectly *drained* conditions, $\dot u = 0$. The volume $\dot V_w$ of pore water squeezed out from the sample can be measured via the pore water system. The corresponding volumetric deformation rate is $\dot\varepsilon_{\mathrm{vol}}^* = \dot V_w/V$. There are two origins, how the water is squeezed out of the sample:

- compression of skeleton due to $\dot\sigma_a > 0$ and $\dot\sigma_r > 0$
- MP due to $\dot\sigma_r > 0$

The apparent volumetric strain rate $\dot\varepsilon_{\mathrm{vol}}^*$ can be decomposed into the true deformation $\dot\varepsilon_{\mathrm{vol}} = \dot\varepsilon_a + 2\dot\varepsilon_r$ of the skeleton and the MP contribution

$$\text{drained: } \dot\varepsilon_{\mathrm{vol}}^* = \dot V_w/V = \dot\varepsilon_{\mathrm{vol}} + \dot\varepsilon_{\mathrm{vol}}^{MP} = \dot\varepsilon_{\mathrm{vol}} + \dot\sigma_r/k_{MP} \tag{4}$$

The true strain rate $\dot\varepsilon_{\mathrm{vol}} = \dot V/V$ is defined using the volume V of the envelope (a cylinder or a barrel), that encompasses all grains, see the green line in Fig. 3a. It turns out that despite undrained conditions and $K_m = \infty$, the true deformation $\dot\varepsilon_{\mathrm{vol}} \neq 0$ is possible.

Under perfectly *undrained* conditions, $\dot V_w = 0$, stress increment $\dot\sigma_r > 0$ may wrinkle the membrane but it cannot shift it. The volume of the closed mass cannot change because of $K_m = \infty$. A closer look at the boundary surface reveals that grains are moved slightly outwards and pore water is pressed slightly inwards the initial boundary surface. It is essential to understand that the *average* boundary surface *need not* be moved for true $\dot\varepsilon_{\mathrm{vol}}$ to occur. Changes in the "amplitude of wrinkles" make the undrained test not exactly isochoric, Fig. 3 a. From Eq. 4 one obtains

$$\text{undrained: } 0 = \dot\varepsilon_{\mathrm{vol}} + \dot\varepsilon_{\mathrm{vol}}^{MP} = \dot\varepsilon_{\mathrm{vol}} + \dot\sigma_r/k_{MP} \tag{5}$$

and hence $\dot\sigma_r > 0$ looses the undrained sample by $\dot\varepsilon_{\mathrm{vol}} = -\dot\varepsilon_{\mathrm{vol}}^{MP} = -\dot\sigma_r/k_{MP}$. It happens despite the incompressibility of the substance. The MP can be seen as connected in series with the constitutive response of the skeleton: the elements have the common stress rate $\dot\sigma_r$ and the additive strain rates given in Eq. (4).

[(1)] For rough estimation of the additional stiffness, the elasticity of the membrane $E_M \approx 2.1$ MPa and the thickness $t_M = 0.3$ mm. Changes of radial strain ε_r of the sample are identical with the strain in the membrane. For a sample of diameter $2r = 100$mm one obtains, according to the boiler formula, $\sigma_r^+ = 2t_M E_M \varepsilon_r/(2r)$. This additional radial stress due to $\varepsilon_r = 10\%$ is $\sigma_r^+ = 1.2$ kPa only. The effect seems negligible indeed.

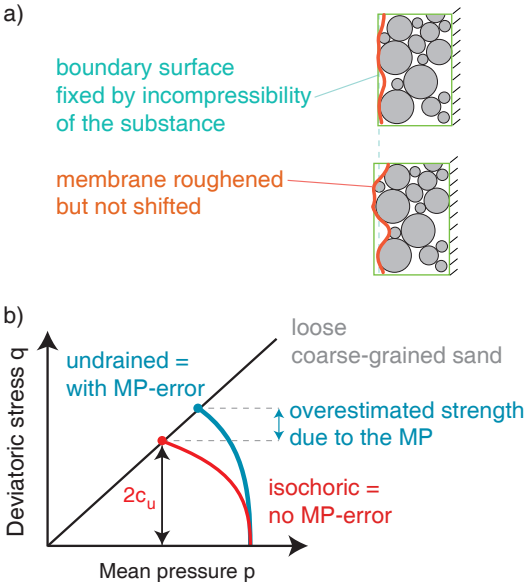

Figure 3. *a) The membrane encompassing an undrained sample with incompressible substance cannot in average be moved. However, grains penetrate into the membrane and the contact surface is roughened. The diameter of a cylinder that encompass all grains increases. b) A triaxial compression test on a loose undrained sand sample.*

During an undrained triaxial compression test, $\dot{q} > 0$, loosely compacted samples show relaxation, $\dot{p} < 0$, due to restricted contractancy. This effect is better known as the pore pressure build-up, and can be quantified by the well known parameter A by Skempton [1954]. Actually, the increase $\dot{u}$ is a consequence of the relaxation and not vice versa[(2)].

The relaxation is a constitutive phenomenon which can be quantified using a dilatancy rule from the literature Rowe [1962], Taylor [1948]. Under undrained conditions, the relaxation $\dot{\sigma}_r < 0$ causes $\dot{\varepsilon}_{\rm vol}^{MP} < 0$ and $\dot{\varepsilon}_{\rm vol} > 0$. Hence, the undrained shear is not isochoric but slightly dilatant. Undrained stress paths reach therefore larger deviatoric stresses compared to the isochoric ones, Fig. 3b. This overestimation of isochoric strength can be dangerous in practice.

3. Removal of the MP-error from the stiffness

In triaxial tests, the MP-error can be evaluated using the rates $\dot{p}, \dot{q}, \dot{\varepsilon}_{\rm vol}, \dot{\varepsilon}_q$ of the well known Roscoe invariants. The MP appears on the lateral surface of the sample only, and hence

$$\dot{\varepsilon}_r^{MP} = \tfrac{1}{2}\dot{\varepsilon}_{\rm vol}^{MP} \quad \text{and} \quad \dot{\varepsilon}_a^{MP} = 0 \tag{6}$$

$$\text{and} \quad \dot{\varepsilon}_q^{MP} = \tfrac{2}{3}(\dot{\varepsilon}_a^{MP} - \dot{\varepsilon}_r^{MP}) = -\tfrac{2}{3}\dot{\varepsilon}_r^{MP} = -\tfrac{1}{3}\dot{\varepsilon}_{\rm vol}^{MP} \tag{7}$$

[(2)]This must be so because effective stress paths under undrained shearing are almost identical as the ones under isochoric shearing of analogous dry samples.

The incremental stiffness can be determined from different stress rates and strain rates applied/measured at the same stress[(3)]. The volume measurement via pore water system gives the apparent values $\dot{\varepsilon}_{\rm vol}^{*} = \dot{\varepsilon}_{\rm vol} + \dot{\varepsilon}_{\rm vol}^{MP}$ and $\dot{\varepsilon}_q^{*} = \dot{\varepsilon}_q + \dot{\varepsilon}_q^{MP}$, which lead to an inexact material stiffness

$$\text{soil + MP:} \quad \begin{Bmatrix} \dot{p} \\ \dot{q} \end{Bmatrix} = \begin{bmatrix} K^* & K_{pq}^* \\ K_{qp}^* & 3G^* \end{bmatrix} \cdot \begin{Bmatrix} \dot{\varepsilon}_{\rm vol} + \dot{\varepsilon}_{\rm vol}^{MP} \\ \dot{\varepsilon}_q + \dot{\varepsilon}_q^{MP} \end{Bmatrix} \tag{8}$$

with

$$\dot{\varepsilon}_{\rm vol}^{MP} = \frac{\dot{\sigma}_r}{k_{MP}} \quad \text{and} \quad \dot{\varepsilon}_q^{MP} = -\frac{\dot{\sigma}_r}{3k_{MP}} \tag{9}$$

and with

$$\dot{\sigma}_r = \dot{p} - \dot{q}/3 \tag{10}$$

The components K^*, K_{pq}^*, K_{qp}^* and G^* are similar to the constitutive components K, K_{pq}, K_{qp} and G but they are blurred by the MP-contributions. Pure constitutive stiffness can be extracted from Eq. 8. In Eq. (8), the MP-error has been *assumed* to appear in strain components only[(4)]. Mathematically, Eq. 8 can be resolved for true constitutive stiffness of the skeleton as follows

$$\begin{Bmatrix} \dot{p} \\ \dot{q} \end{Bmatrix} = \begin{bmatrix} K & K_{pq} \\ K_{qp} & 3G \end{bmatrix} \cdot \begin{Bmatrix} \dot{\varepsilon}_{\rm vol} \\ \dot{\varepsilon}_q \end{Bmatrix} \tag{11}$$

with the full form of stiffness

$$\frac{1}{A^*} \left[\begin{array}{c|c} G^*K^* - 3k_{MP}K^* - K_{pq}^*K_{qp}^*/3 & 3G^*K^* - K_{pq}^*(3k_{MP} + K_{qp}^*) \\ 3G^*K^* - (3k_{MP} + K_{pq}^*)K_{qp}^* & 9G^*(K^* - k_{MP}) - 3K_{pq}^*K_{qp}^* \end{array}\right]$$

and wherein $A^* = G^* - 3k_{MP} + 3K^* - K_{pq}^* - K_{qp}^*$. A perfect test without the MP corresponds to the limit $k_{MP} \to \infty$. Similarly, one may find the full form of the matrix used in Eq. 8

$$\begin{bmatrix} K^* & K_{pq}^* \\ K_{qp}^* & 3G^* \end{bmatrix} = \tag{12}$$

$$\frac{1}{A} \left[\begin{array}{c|c} GK + 3k_{MP}K - K_{pq}K_{qp}/3 & 3GK + 3k_{MP}K_{pq} - K_{pq}K_{qp} \\ 3GK + 3k_{MP}K_{qp} - K_{pq}K_{qp} & 9Gk_{MP} + 9GK - 3K_{pq}K_{qp} \end{array}\right]$$

wherein $A = G + 3k_{MP} + 3K - K_{pq} - K_{qp}$. Eqs. 11 and 12 can be easily derived with the MATHEMATICA, Script 1, Appendix C. The components $K^*, G^*, \ldots$ are denoted as `K,G ...` and $K, G, \ldots$ as `Ke,Ge ...` in the Script 1.

4. Correction of stress paths

The influence of the MP is evaluated for isotropic compression and for undrained stress paths. In both cases, the correction is derived for the special case of incompressible substance $K_m = \infty$, and extend the formulas for $K_m < \infty$. In one case the correction of the measured stress path is not necessary.

[(3)]Some authors Gudehus [1979], Knittel et al. [2020] prefer to use the so-called stress envelope to describe such incremental response.

[(4)]Actually, the stress measurement can also be affected because the axial force is divided by an inexact horizontal cross-section of the sample. Using the nominal effective stress that relates current loading to the initial geometry of the sample one could argue that no such "assumption" is needed. However, to be exact, radial stress σ_r should always be interpreted as a Cauchy stress component.

4.1. Undrained isotropic compression with $K_m = \infty$, no effect of the MP

A sample with isotropic elastic stiffness is examined under undrained, isotropic compression with $\dot{p}^{\rm tot} > 0$ and $\dot{q}^{\rm tot} = \dot{q} = 0$. The substance is incompressible. From $\dot{V}_w = 0$ or $\dot{\varepsilon}^*_{\rm vol} = 0$, one finds $\dot{\varepsilon}_{\rm vol} = -\dot{\sigma}_r/k_{MP}$ and $\dot{\varepsilon}_q = \dot{\varepsilon}^*_q + \dot{\sigma}_r/(3k_{MP})$. From Eq. 10 with $\dot{q} = 0$, one obtains simply $\dot{\sigma}_r = \dot{p}$

$$\left\{\begin{matrix}\dot{p}\\ 0\end{matrix}\right\} = \left[\begin{matrix}K & 0\\ 0 & 3G\end{matrix}\right]\cdot\left\{\begin{matrix}-\dot{p}/k_{MP}\\ \dot{\varepsilon}^*_q + \dot{p}/(3k_{MP})\end{matrix}\right\} \tag{13}$$

From the first line, it follows[5] that $\dot{p} = 0$ and from the second line $\dot{\varepsilon}^*_q = 0$. In consequence, $\dot{u} = \dot{p}^{\rm tot}$ and the MP for $\dot{p} = \dot{\sigma}_r = 0$ has no effect. In the more general case,

$$\left\{\begin{matrix}\dot{p}\\ 0\end{matrix}\right\} = \left[\begin{matrix}K & K_{pq}\\ K_{qp} & 3G\end{matrix}\right]\cdot\left\{\begin{matrix}-\dot{p}/k_{MP}\\ \dot{\varepsilon}^*_q + \dot{p}/(3k_{MP})\end{matrix}\right\} \tag{14}$$

$$\text{with}\quad \det\left[\begin{matrix}-K - k_{MP} & K_{pq}\ k_{MP}\\ -K_{qp} & 3G\ k_{MP}\end{matrix}\right] \neq 0, \tag{15}$$

one can also obtain the solution $\dot{p} = 0$ and $\dot{\varepsilon}^*_q = 0$ with identical consequences as before. Formally, however, the singularity should be excluded, see Eq. 15.

4.2. Correction of undrained stress paths for the MP at $K_m = \infty$

Consider an undrained triaxial compression test with $\dot{q} > 0$ and a simple, incrementally linear constitutive relation with the well known elastic constants K, G supplemented by the coupling term K_{pq} between $\dot{p}$ and $\dot{\varepsilon}_q$.

$$\text{isochoric:}\quad \left\{\begin{matrix}\dot{p}\\ \dot{q}\end{matrix}\right\} = \left[\begin{matrix}K & K_{pq}\\ 0 & 3G\end{matrix}\right]\cdot\left\{\begin{matrix}0\\ \dot{\varepsilon}_q\end{matrix}\right\} \tag{16}$$

In comparison to Eq. (11), the simplification $K_{qp} = 0$ is assumed. The coupling term K_{pq} depends on the stress ratio q/p, on the void ratio e and on the sign of $\dot{q}$. This component can be analytically quantified with the Skempton's equation $\dot{u} = B\left(\dot{\sigma}^{\rm tot}_r + A_S(\dot{\sigma}_a - \dot{\sigma}_r)\right)$ for isochoric conditions. It is of advantage to modify this original formula using $A = B(A_S - \frac{1}{3})$ and make it also valid for triaxial extension

$$\dot{u} = B\dot{p}^{\rm tot} + A|\dot{q}| \tag{17}$$

Using $B = 1$ (i.e. $K_m = \infty$), Eq. (17) can be simplified to $A|\dot{q}| = -\dot{p}$ and comparing this to Eq. 16 one obtains

$$K_{pq} = -3GA\ \text{sign}(\dot{q}) \tag{18}$$

Alternatively, one of the well established dilatancy rules after Rowe [1962] or after Taylor [1948] can be used. For example, the Taylor dilatancy rule yields

$$K_{pq} = K(q/p - \sqrt{6}M/2) \tag{19}$$

$$\text{with}\quad M = \begin{cases} M_C = \frac{6\sin\varphi}{3-\sin\varphi} & \text{for}\quad \dot{\varepsilon}_q > 0\\ M_E = -\frac{6\sin\varphi}{3+\sin\varphi} & \text{for}\quad \dot{\varepsilon}_q < 0\end{cases} \tag{20}$$

In the lab, K_{pq} can be obtained from $K^*_{pq}, K^*_{qp}, G^*, K^*$ and from k_{MP} using Eq. 11.

[5] The special case with $K/k_{MP} = -1$ is not realistic

The inclination $\dot{p}/\dot{q}$ of the stress path from Eq. 16 for isochoric conditions can be compared with $\dot{p}/\dot{q}$ from

$$\text{undrained:}\quad \left\{\begin{matrix}\dot{p}\\ \dot{q}\end{matrix}\right\} = \left[\begin{matrix}K & K_{pq}\\ 0 & 3G\end{matrix}\right]\cdot\left\{\begin{matrix}-\dot{\sigma}_r/k_{MP}\\ \dot{\varepsilon}^*_q + \frac{1}{3}\dot{\sigma}_r/k_{MP}\end{matrix}\right\}, \tag{21}$$

wherein $\dot{\sigma}_r = \dot{p} - \frac{\dot{q}}{3}$. The true skeleton deformations are $\dot{\varepsilon}_{\rm vol} = -\dot{\varepsilon}^{MP}_{\rm vol} = -\dot{\sigma}_r/k_{MP}$ and $\dot{\varepsilon}_q = \dot{\varepsilon}^*_q - \dot{\varepsilon}^{MP}_q = \dot{\varepsilon}^*_q + \dot{\sigma}_r/(3k_{MP})$, wherein $\dot{\varepsilon}^*_q$ is the non-purified deviatoric strain rate. From (16) and from (21) one obtains

$$\left.\frac{\dot{p}}{\dot{q}}\right|_{\rm isochoric} = \frac{K_{pq}}{3G}\ \text{and}\ \left.\frac{\dot{p}}{\dot{q}}\right|_{\rm undrained} = \frac{GK + k_{MP}K_{pq}}{3G(K + k_{MP})}, \tag{22}$$

respectively. The undrained inclination from Eq. $(22)_2$ is steeper than the isochoric inclination from Eq. $(22)_1$ because $K_{pq} < 0$. Eq. $(22)_2$ corresponds to the ratio $K^*_{pq}/(3G^*)$ if expressed with true material components of stiffness from Eq.12 and with $K_{qp} = 0$, see Fig. 4.

Equations $(21)_2$ and $(22)_2$ can be easily derived with MATHEMATICA in Appendix C, Script 2. The measured inclination from Eq. $(22)_2$ is denoted as $h = \dot{p}/\dot{q}$. The purified (without the MP) inclination $h_0 = \dot{p}/\dot{q}|_{\rm isochoric}$ from $(22)_1$ can be easily calculated (for each increment) from $(22)_2$ using

$$h_0 = h + \beta(h - \frac{1}{3}) \quad \text{with} \quad \beta = K/k_{MP} \tag{23}$$

The MATHEMATICA derivation is straightforward (Appendix C, Script 3). A given undrained stress path can be converted to the isochoric one using (23) increment by increment. True isochoric paths are of practical interest and hence (23) is of importance. In Section 4.4, this conversion rule will be extended to the MP with compressible substance, $K_m < \infty$.

In the following example, a cyclic stress path, `stateU`, is generated analytically. It will be treated as if it were an "undrained" path measured in the lab and needed a correction to the isochoric path. The increments $\{\dot{p}, \dot{q}\}$ with inclinations $h = \dot{p}/\dot{q}$ are given. One calculates h_0 from (23) preserving the deviatoric components $\dot{q}$, i.e. only the pressure increments $\dot{p} = h_0\dot{q}$ are modified. Finally, the corrected isochoric path is written, `stateI`, and both paths are plotted for comparison (MATHEMATICA in Appendix C, Script 4).

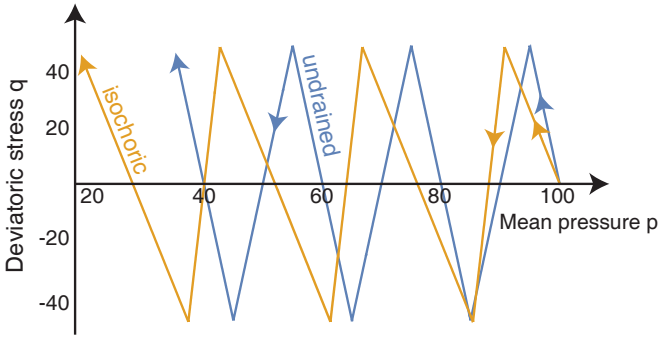

Figure 4. *"Measured" undrained stress path and corrected isochoric stress path. For simplicity, the bulk stiffness K of the skeleton and k_{MP} are assumed constant in this example.*

Note that the undrained triaxial compression $\dot{\varepsilon}_q > 0$ needs a stronger correction than the undrained triaxial extension $\dot{\varepsilon}_q < 0$. According to (23), for $h = \frac{1}{3}$ one obtains $h = h_0$ and no correction is needed. Indeed, a triaxial compression with the inclination $\dot{p}/\dot{q} = \frac{1}{3}$ corresponds to $\dot{\sigma}_a > 0$ and $\dot{\sigma}_r = 0$. According to Eq. 2 no MP effects appear at $\dot{\sigma}_r = 0$.

4.3. Isotropic compression with $K_m < \infty$, Skempton parameter B

A good starting point for the analysis of compressible soils is a poorly drained test in which the pore pressure can change. The increase of pore pressure, $\dot{u} > 0$, at $K_m < \infty$ reduces the relative volume $\dot{V}_w/V$ of water squeezed out from the sample by $\dot{u}/K_m$. This can be taken into account in Eq. 4 as follows,

$$\dot{V}_w/V = \dot{\varepsilon}_{\text{vol}} + \dot{\sigma}_r/k_{MP} - \dot{u}/K_m \tag{24}$$

The deformation of the substance is assumed[6] to be $\dot{u}/K_m$. The bulk modulus of the substance is

$$K_m = [n(1-S_r)/K_a + nS_r/K_w + (1-n)/K_s]^{-1} \tag{25}$$
$$\text{with} \quad K_w \approx 2.2\text{GPa} \quad \text{and} \quad K_s \approx 50\text{GPa}$$

From the general Equation 24, one can easily obtain the perfectly undrained condition, $\dot{V}_w = 0$, or perfectly drained condition, $\dot{u} = 0$, as special cases.

Undrained *isotropic compression* tests, $\dot{q} = \dot{q}^{\text{tot}} = 0$, with incompressible substance $K_m = \infty$ have been already discussed in Section 4.1. It could be concluded, that no MP appears, $\dot{\sigma}_r = \dot{p} = 0$, and that the Skempton parameter is $B = \dot{u}/\dot{p}^{\text{tot}} = 1$. However, even a small number of little gas bubbles renders the substance compressible, $K_m < \infty$. In this case, the MP can affect Skempton parameter B, and therefore the B-test will be examined in more detail here.

The most important component of K_m is stiffness of the air $K_a \approx u_a \approx u + u_{\text{atm}}$. For fast loading, one may consider using the adiabatic stiffness $K_a = \frac{7}{5}u_a$. In small air bubbles, the absolute air pressure u_a can be much higher than the absolute water pressure, $u_w = u + u_{\text{atm}}$. This can be quantified with the Young-Laplace equation $u_a = u_w + \frac{2}{r_a}\gamma_{a/w}$, where r_a is the radius of the bubble and $\gamma_{a/w} \approx 73 \cdot 10^{-3}$ N/m is the surface tension. Additionally, one can take into account the solvability (Henry's law) and diffusion of air in water. In the incremental stress-strain relation, $K_m = \text{const}$ is assumed.

An *undrained* isotropic compression (a so-called B-Test) corresponds to $\dot{p}^{\text{tot}} > 0$, $\dot{q}^{\text{tot}} = \dot{q} = 0$ and $\dot{V}_w = 0$. From (24) with $\dot{V}_w = 0$ and $\dot{\sigma}_r = \dot{p} - \frac{1}{3}\dot{q} = \dot{p}$ one obtains

$$0 = \dot{\varepsilon}_{\text{vol}} + \dot{\varepsilon}^{\text{MP}} - \dot{u}/K_m \quad \text{or} \quad \dot{u}/K_m = \dot{p}/k_{\text{MP}} + \dot{p}/K \tag{26}$$

Now, the definition of the Skempton parameter B can be used: one substitutes $\dot{u} = B\dot{p}^{\text{tot}}$ and $\dot{p} = (1-B)\dot{p}^{\text{tot}}$ into $(26)_2$ and then eliminates $\dot{p}^{\text{tot}} = \dot{p} + \dot{u}$. This leads to the following expression

$$B = \frac{K_m(K + k_{MP})}{KK_m + Kk_{MP} + K_m k_{MP}} \tag{27}$$

[6] By this assumption, the small volumetric deformation $\dot{p}/K_s$ of individual grains due to *effective* pressure are disregarded.

At the limit $k_{MP} \to \infty$, the well known formula $B = K_m/(K + K_m) = \dot{u}/(\dot{u} + \dot{p})$ is recovered, which corresponds to equal volumetric deformation rates of the skeleton and the substance. At the limit $K_m \to \infty$, the Skempton parameter is $B = 1$, independently of k_{MP}.

For completeness, the isotropic compression under *drained* conditions is considered: $\dot{p}^{\text{tot}} > 0$ and $\dot{q}^{\text{tot}} = \dot{q} = 0$, $\dot{u} = 0$, but also $\dot{p}^{\text{tot}} = \dot{p} = \dot{\sigma}_r$. Moreover, the substance cannot be deformed, $\dot{u}/K_m = 0$. In this case

$$\dot{\varepsilon}^*_{\text{vol}} = \dot{V}_w/V = \dot{p}/K + \dot{p}/k_{\text{MP}} \tag{28}$$

holds. The true volumetric strain of the skeleton is $\dot{\varepsilon}_{\text{vol}} = \dot{p}/K$, of course.

4.4. Correction of undrained stress paths for the MP at $K_m < \infty$

Using the volumetric strain measured via the pore water system and having $K_m < \infty$, one observes the following inexact strain rates

$$\dot{\varepsilon}^*_{\text{vol}} = \frac{\dot{V}_w}{V} = \dot{\varepsilon}_{\text{vol}} + \dot{\sigma}_r/k_{MP} - \dot{u}/K_m \tag{29}$$

$$\text{and} \quad \dot{\varepsilon}^*_q = \dot{\varepsilon}_q - \frac{\dot{\sigma}_r}{3k_{MP}}, \tag{30}$$

wherein $\dot{\varepsilon}_{\text{vol}}$ and $\dot{\varepsilon}_q$ are true deformations of the skeleton, see Eqs. 8 and 24. Note that K_m affects equally ε^*_a and ε^*_r and hence, contrarily to k_{MP}, stiffness K_m does not affect $\dot{\varepsilon}^*_q$. The corresponding (not constitutive) stress-strain relations are

$$\begin{Bmatrix} \dot{p} \\ \dot{q} \end{Bmatrix} = \begin{bmatrix} K^* & K^*_{pq} \\ K^*_{qp} & 3G^* \end{bmatrix} \cdot \begin{Bmatrix} \dot{\varepsilon}_{\text{vol}} + \dot{\sigma}_r/k_{MP} - \dot{u}/K_m \\ \dot{\varepsilon}_q - \frac{1}{3}\dot{\sigma}_r/k_{MP} \end{Bmatrix}, \tag{31}$$

wherein $\dot{\sigma}_r = \dot{p} - \frac{\dot{q}}{3}$. As in the previous section, the inclination $h = \dot{p}/\dot{q}$ can be determined for the special case of $K_{qp} = 0$ under undrained conditions, $\dot{V}_w = 0$, i.e. $\dot{\varepsilon}^*_{\text{vol}} = 0$. Additionally, it is assumed that the cell pressure does not change,

$$\dot{u} + \dot{\sigma}_r = \dot{\sigma}^{\text{tot}}_r = 0 \quad \text{or} \quad \dot{u} = -\dot{\sigma}_r \tag{32}$$

With these assumptions, the true constitutive relation can be written in the form

$$\begin{Bmatrix} \dot{p} \\ \dot{q} \end{Bmatrix} = \begin{bmatrix} K & K_{pq} \\ K_{qp} & 3G \end{bmatrix} \cdot \begin{Bmatrix} -\dot{\sigma}_r/k_{MP} + \dot{u}/K_m \\ \dot{\varepsilon}^*_q + \frac{1}{3}\dot{\sigma}_r/k_{MP} \end{Bmatrix}$$
$$= \begin{bmatrix} K & K_{pq} \\ 0 & 3G \end{bmatrix} \cdot \begin{Bmatrix} -\dot{\sigma}_r/\bar{k} \\ \dot{\varepsilon}^*_q + \frac{1}{3}\dot{\sigma}_r/k_{MP} \end{Bmatrix} \tag{33}$$

with the abbreviation $1/\bar{k} = 1/k_{MP} + 1/K_m$. Similarly as in the previous section, one obtains

$$\left.\frac{\dot{p}}{\dot{q}}\right|_{\text{isochoric}} = \frac{K_{pq}}{3G} \quad \text{and} \quad \left.\frac{\dot{p}}{\dot{q}}\right|_{\text{undrained}} = \frac{GK + \bar{k}K_{pq}}{3G(K + \bar{k})} \tag{34}$$

and hence the purified inclination is

$$h_0 = h + \beta_m(h - \frac{1}{3}) \quad \text{with} \quad \beta_m = \frac{K}{\bar{k}} = \frac{K}{k_{MP}} + \frac{K}{K_m} \tag{35}$$

5. Recommended correction for undrained cyclic tests

In the previous section, the effect of the MP was discussed for individual stress increments. Here, a complete correction

procedure is presented for an undrained cyclic test. Interpretation of these tests was actually the motivation for the whole research project. Unfortunately, the knowledge of the stress path and the membrane does not suffice to apply the correction. Difficulties arise from the variability of the effective bulk modulus of soil $K(p)$ and $k_{MP}(p)$ with effective pressure p.

According to Eq. 23 or Eq. 35 the correction from h to h_0, depends on $\beta(p)$. The problem arises at $p \to 0$, i.e. shortly before liquefaction, during the so-called cyclic mobility. For simplicity in this paragraph, nearly isotropic conditions, $p \approx \sigma_r$, are assumed. The limit of

$$\beta = \frac{K(p)}{k_{MP}(p)} \sim \frac{p^{n_K}}{p^{n_k}} = p^{n_K - n_k} \tag{36}$$

at $p \to 0$ depends upon empirical formulas used. From (40) one obtains after Nicholson et al. [1993] $k_{MP} \sim p^{n_k}$ with $n_k = 1$. This exponent is only $n_k = \frac{2}{3}$ if obtained from (43) after Baldi and Nova [1984]. The constitutive bulk modulus of sand skeleton can be approximated by

$$K(p) = \frac{(1+e)h_B \left(\frac{3p}{h_B}\right)^{1-n_B}}{3en_B} \tag{37}$$

with the material constants[7] $n_B \approx 0.2$ and $h_B \approx 3 \cdot 10^9$kPa after Bauer [1992]. Hence $K \sim p^{n_K}$ with $n_K = \frac{4}{5}$ has an exponent that can be larger or smaller than n_k.

The combination of Eq. (37) with k_{MP} by Nicholson et al. [1993] leads to huge corrections

$$\lim_{p\to 0} \beta = \lim_{p\to 0} p^{n_K - n_k} \approx \lim_{p\to 0} p^{-1/5} = \infty \tag{38}$$

but using Eq. (37) with k_{MP} by Baldi and Nova [1984] the analogous correction dwindles, $\beta \to 0$. Evidently, inaccurate description of $K(p)$ and $k_{MP}(p)$ may dominate and fully blur the MP-correction procedure at small pressures.

It seems reasonable to reduce the MP-correction at small p irrespectively of the exponents n_k and n_K used in $k_{MP} \sim p^{n_k}$ and $K \sim p^{n_K}$. At very small values of p this correction is of secondary importance for practical applications. Therefore a redefinition of the liquefaction point is proposed. The conventional definition of cyclic liquefaction is based on the strain amplitude which is required to surpass $\varepsilon_q^{\text{ampl}} = 10\%$, cf. Lee and Fitton [1969], Towhata [2008], Wichtmann et al. [2019] (some authors propose even $2\varepsilon_q^{\text{ampl}} = 15\%$). However, before $2\varepsilon_q^{\text{ampl}} = 10\%$ is attained, several nearly large cycles need to be applied.

In order to mitigate this problem, the "increased mobility" cycles can be simply cropped and thus eliminated from the correction procedure. For this purpose, we propose the following inequality as a redefinition of the point of cyclic liquefaction

$$p < 0.5\, q^{\text{ampl}}/M_e \quad \text{with} \quad M_e = 6\sin\varphi/(3+\sin\varphi) \tag{39}$$

[7] The granular hardness $h_B \approx 3 \cdot 10^9$kPa was measured upon the isotropic unloading. A much smaller granular hardness $h_B \approx 3 \cdot 10^7$ kPa is obtained from first loading compression tests and this standard value is usually given in the literature. Using such h_B in Eq. (37) one should increase the resulting $K(p)$ roughly by a factor 2.5. It follows from the proportionality $K \sim h_B^{n_B}$, cf. Eq. (37). An increase of K by factor $2.5 \approx 100^{0.2}$ corresponds to a factor 100 at h_B.

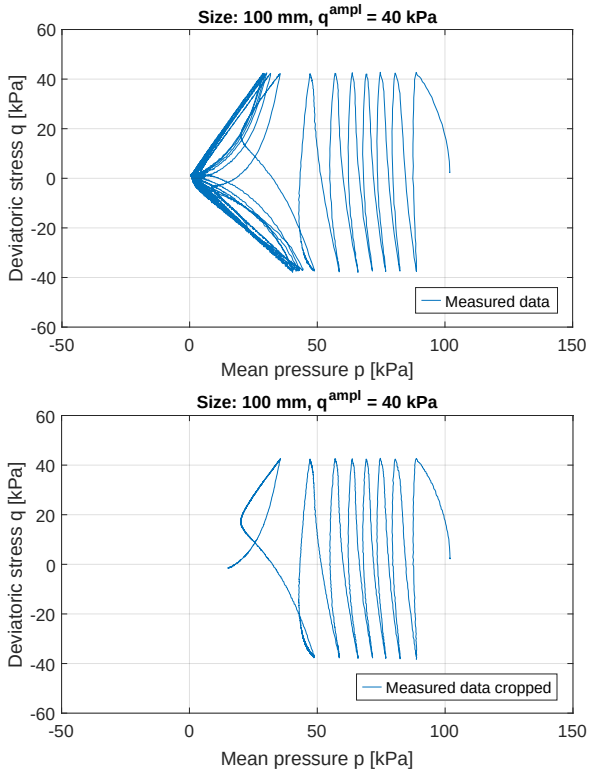

Figure 5. *An undrained cyclic test* continued up to $\varepsilon_q^{\text{ampl}} = 10\%$ and cropped just after the condition (39) is reached.

In consequence of Eq. 39, the liquefaction occurs earlier, i.e. after a smaller number of cycles N_f or, equivalently, at slightly smaller CRR, Fig.5. Using the definition of Eq. 39 the final effect of the MP-correction causes still a substantial reduction [8] of the CRR-value of soil as shown in Fig. 8.

The correction procedure of the undrained data (obtained from the lab) can be summarized in the following flow-chart

(1) Input of the measured stress path
(2) Evaluation of the bulk stiffness K of skeleton. Usually $K(p,e)$ is a barotropic function of the current effective pressure. Eq. (37) was originally proposed by Bauer [1992] and is commonly used in hypoplastic constitutive models, such as Wolffersdorff [1996], as a stiffness upon first loading. This $K(p)$ should be increased roughly by a factor two[9]. In Appendix D, the unloading portion of the compression curve is used for the calibration of h_B and n_B, Fig. 11 below. No increase of stiffness is required in such case.
(3) The bulk modulus K from Eq. (37) is known to be overly stiff for small pressures, $p < 25$ kPa. Using the factor $\zeta = (1-\exp(-p/p_Z))^{Z-n_B}$ proposed by Osinov et al. [2016], the reduced stiffness is $\bar{K} = K\zeta$. The correction with $Z = 2$ and $p_z = 25$ kPa is shown in Fig. 7.

[8] Hence the modification of $K(p)$ in the step (3) of the flow-chart.

[9] The relaxation corresponds to unloading which is approximately twice stiffer

(4) At first, the start point (p_0^c, q_0^c) of the corrected path is set to the actual start point (p_0, q_0) of the measured path.

(5) For each increment: values of σ_r, p are read and the MP coefficient $k_{MP} = \frac{\sigma_r}{S^{MP} A_{\text{mem}}/V_0}$ is evaluated, see Appendix B. The correction factor $\beta = \bar{K}/k_{MP}$ is evaluated for the current p, e. The corrected stress increment is $\dot{q}^c = \dot{q}$ and $\dot{p}^c = \dot{p} + \beta(\dot{p} - \dot{q}/3)$. After the update, the corrected stress is $q^c = q^c + \dot{q}^c \Delta t$, $p^c = p^c + \dot{p}^c$.

(6) The incremental correction is continued until the measured stress path reaches the liquefaction $p_{\min} \leqslant 0.5 q^{\text{ampl}}/M_e$. After this condition[10] is satisfied, the procedure is stopped.

(7) The final, corrected p^c (after all cycles) is always smaller than the final p. The corresponding difference, $\Delta p = p - p^c > 0$, is added to the corrected path, Fig. 6, and thus this path is shifted along the p-axis to the right. The end-points of both measured and corrected paths coincide but the starting point of the corrected path is artificially increased beyond p_0.

(8) The original cyclic resistance is $\text{CRR} = \frac{1}{2} q^{\text{ampl}}/p_0$ and the corrected one is $\text{CRR}^c = \frac{1}{2} q^{\text{ampl}}/p_0^c$. As shown in Fig. 8-bottom-left, the corrected value is much smaller.

For details on the performed test see Appendix A and the MATHEMATICA source code of the correction procedure is given in Appendix C.

6. Discussion

The portion of corrected stress path beyond the failure line or in the tensile zone is completely fictitious, of course, and may seem counterintuitive. The fictitious (shifted) starting point p_0 is also challengeable because the true behaviour of the sample in the vicinity of the increased p_0 is unknown. Therefore, two alternative ideas could be considered in future:

One alternative evaluation of undrained cyclic tests for CRR could be:
(1) conduct several undrained cyclic tests with different ratios $\frac{1}{2} q^{\text{ampl}}/p_0$
(2) correct each path
(3) crop the corrected paths at liquefaction[11]
(4) count the number of cycles N of each cropped path
(5) interpolate between corrected N values in order to obtain $\text{CRR} = \frac{1}{2} q^{\text{ampl}}/p_0$ at exactly $N = N_f = 10$
In comparison to this, an advantage of the "shift p_0"-method is its applicability to a *single* undrained cyclic test with $N = 10$.

The second alternative is suitable especially for large MP-corrections. It needs a *single* undrained cyclic test only:

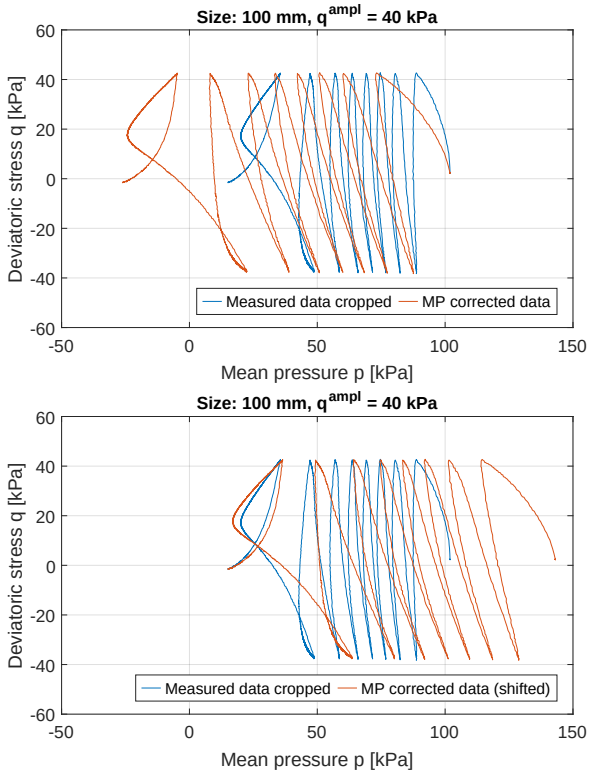

Figure 6. *After the MP-correction, the isochoric stress path is shifted so that both final states p and p^c just satisfy the liquefaction condition (39). The shifted value of p_0^c enters the corrected value $CRR = \frac{1}{2} q^{\text{ampl}}/p_0^c$.*

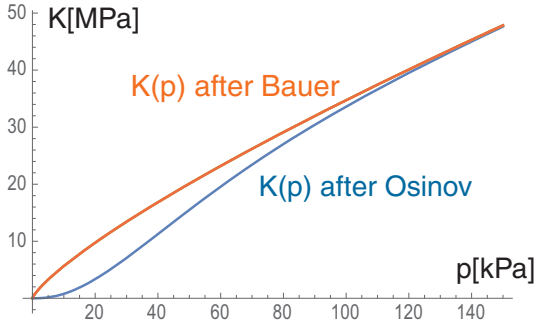

Figure 7. *Original stiffness $K(p)$ after Bauer [1992] should be slightly reduced according to Osinov et al. [2016]. This reduction improves the MP correction at the limit $p \to 0$.*

(1) choose several starting points p_0 on the originally measured stress path
(2) perform the MP-corrections starting from these p_0 points until the corrected path surpass the failure line.
(2) count the cycles N to failure of each corrected path
(3) interpret these numbers N and the respective ratios $\frac{1}{2} q^{\text{ampl}}/p_0$ as if they were obtained from independent tests.
(4) interpolate between corrected N values in order to obtain $\text{CRR} = \frac{1}{2} q^{\text{ampl}}/p_0$ at exactly $N = N_f = 10$
This method assumes that the pre-cycles do not affect the subsequent pore pressure build up, which is disputable.

[10] Using the liquefaction criterion $\varepsilon_q^{\text{ampl}} = 10\%$ would render the correction of CRR overly sensitive to the small stiffness parameters Z and p_Z from the factor ζ.

[11] Where the corrected stress violates the failure criterion for the first time.

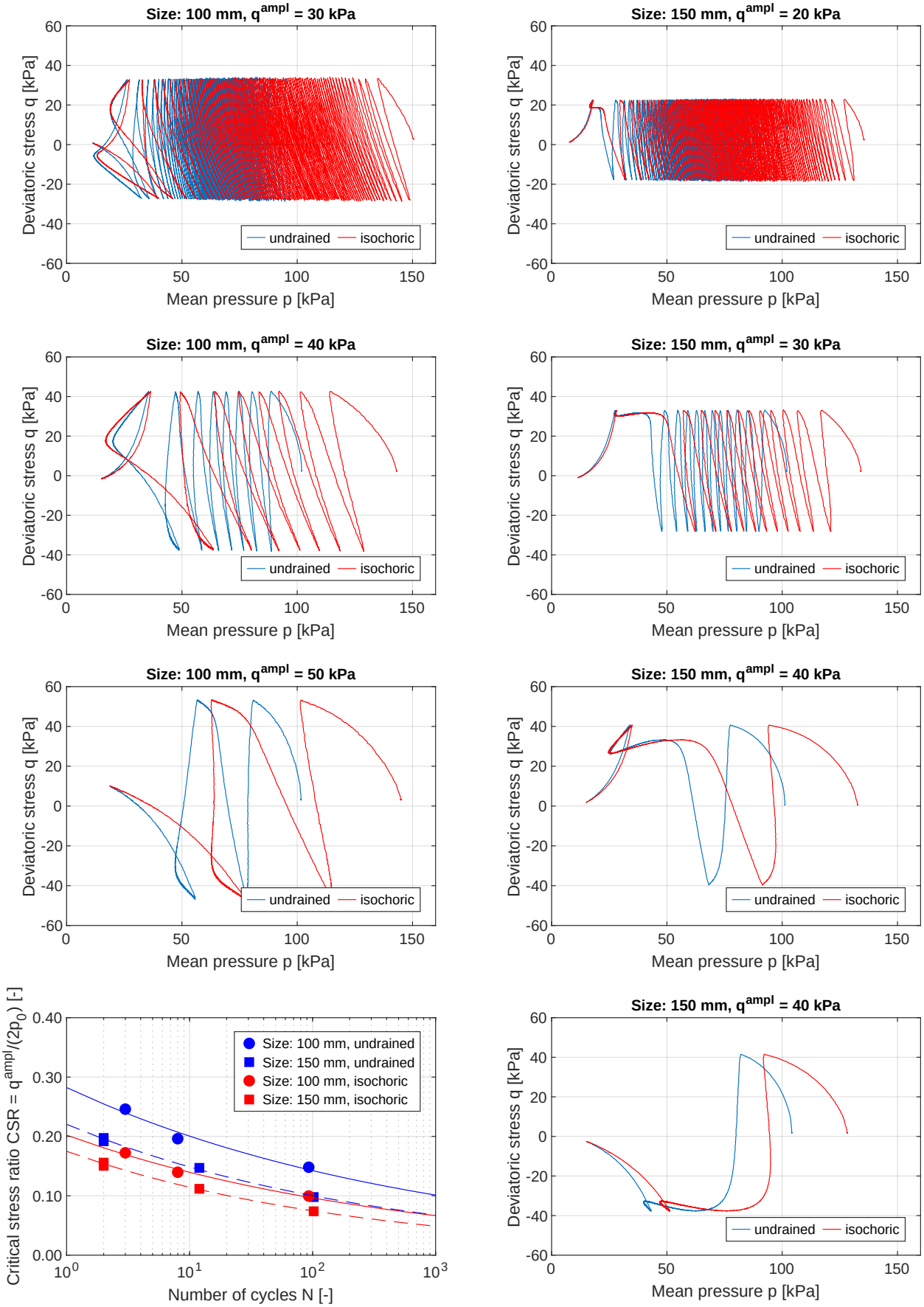

Figure 8. *Measured and MP-corrected undrained paths from stress cycles. The red isochoric line should coincide because pure CRR-results should not depend on the size of the sample.*

7. Conclusions

The MP-error from the triaxial tests can be of importance even for medium-coarse sand. An MP-correction procedure has been proposed to operate on the monotonic or cyclic undrained stress paths obtained from the lab. Beside the measured stress path, two functions should be provided for the MP-correction: the bulk modulus of skeleton $K(p,q)$ and the stiffness of the membrane $k_{MP}(p,q)$. In the case of poor saturation, the stiffness of the substance should also be considered via $K_m(p,q)$. At the limit $p \to 0$, the ratio K/k_{MP} may strongly increase causing unrealistic MP-corrections. In such cases a redefinition of Eq. 39 for the point of liquefaction can be considered.

Conflicts of Interest

The authors see no potential conflicts of interest due to publishing of this paper. The complete review history is available online.

Acknowledgements

The authors are grateful to I. Kimmig for his support. The tests have been performed by H. Borowski and P. Gölz in the laboratory of the Institute for Soil- and Rock Mechanics in Karlsruhe, Germany. The Authors are also indebted to the Reviewers, who rightly suspected a rough error in the material parameters in the first version of the manuscript. This error has been corrected in the last version of the manuscript.

References

Ansal, A. and Erken, A. (1996). Post correction procedure for membrane compliance effects on pore pressure. *Journal of Geotechnical Engineering*, 122(1):27–38. https://doi.org/10.1061/(ASCE)0733-9410(1996)122:1(27).

Baldi, G. and Nova, R. (1984). Membrane penetration effects in triaxial testing. *Journal of Geotechnical Engineering*, 110(3):403–420. https://doi.org/10.1061/(ASCE)0733-9410(1984)110:3(403).

Bauer, E. (1992). *Zum mechanischen Verhalten granularer Stoffe unter vorwiegend ödometrischer Beanspruchung*. PhD thesis, Institut für Boden- und Felsmechanik der Universität Karlsruhe. Heft Nr 130.

Frydman, S., Zeitlen, J., and Alpan, I. (1973). The membrane effect in triaxial testing on granular soils. *Journal of Testing and Evaluation*, 1:37–41. https://doi.org/10.1520/JTE11599J.

Gudehus, G. (1979). Comparison of some constitutive laws for soils under radially symmetric loading and unloading. In *Numerical Methods in Geomechanics*, pages 1309–1323. Balkema, Rotterdam. 3-rd International Conference in Aachen.

Haeri, S. and Shakeri, M. (2010). Effects of membrane compliance on pore water pressure generation in gravelly sands under cyclic loading. *Geotechnical Testing Journal*, 33(5):1–10. https://doi.org/10.1520/GTJ102433.

Kiekbusch, M. and Schuppener, B. (1977). Membrane penetration and its effects on pore pressure. *Journal of the Geotechnical Engineering Division, ASCE*, 103(GT11):1267–1279.

Knittel, L., Wichtmann, T., Niemunis, A., Huber, G., Espino, E., and Triantafyllidis, T. (2020). Pure elastic stiffness of sand represented by response envelopes derived from cyclic triaxial tests with local strain measurements. *Acta Geotechnica*. https://doi.org/10.1007/s11440-019-00893-9.

Lee, K. and Fitton, J. (1969). Factors affecting the cyclic loading strength of soil. In *Vibration Effects of Earthqakes on Soils and Foundations, ASTM Special Technical Publication 450*, pages 71–95.

Newland, P. and Alley, B. (1957). Volume changes during drained triaxial tests on granular materials. *Geotechnique*, 7:17–34. https://doi.org/10.1680/geot.1957.7.1.17.

Nicholson, P. G., Seed, R. B., and Anwar, H. A. (1993). Elimination of membrane compliance in undrained triaxial testing. 1. measurement and evaluation. *Canadian Geotechnical Journal*, 30:727–738. https://doi.org/10.1139/t93-065.

Osinov, V., Chrispoulos, S., and Grandas-Tavera, C. (2016). Vibration-Induced Stress Changes in Saturated Soil: A High Cyclic Problem. In Triantafyllidis, T., editor, *Holistic simulation of geotechnical installation processes. Numerical and physical modelling.*, pages 69–84. Springer. https://doi.org/10.1007/978-3-319-18170-7.

Raju, V. and Sadasivian, S. (1974). Membrane penetration in triaxial tests on sand. *Journal of the Geotechnical Engineering Division, ASCE*, 100(GT4):482–489.

Raju, V. and Venkatramana, K. (1980). Undrained triaxial tests to assess liquefaction potential of sands - effects of membrane penetration. In *Proc. of the International Symposium on Soils under Cyclic Transient Loading, Rotterdam*, volume 2, pages 483–494.

Ramana, K. and Raju, V. (1982). Membrane penetration in triaxial tests. *Journal of Geotechnical Engineering*, 108(2):305–310. https://doi.org/10.1061/(ASCE)0733-9410(1983)109:2(277).

Roscoe, K. H., Schofield, A., and Thurairaja, A. (1963). An evaluation of test data for selecting a yield criterion for soil. In *Proceedings of Laboratory Shear Testing of Soils, Special Technical Publication*, volume 361, pages 111–128. https://doi.org/10.1520/STP29988S.

Rowe, P. (1962). The stress-dilatancy relation for static equilibrium of an assembly of particles in contact. *Proceedings of the Royal Society of London*, 269:500–527. https://doi.org/10.1098/rspa.1962.0193.

Seed, R., Anwar, H., and Nicholson, P. (1989). Evaluation and mitigation of membrane compliance effects in undrained testing of saturated soils. Technical Report Technical report, SU/GT/89-01, Stanford University.

Skempton, A. (1954). The pore pressure coefficients A and B. *Géotechnique*, 4(4):143–147. https://doi.org/10.1680/geot.1954.4.4.143.

Taylor, D. (1948). *Fundamentals of Soil Mechanics*. John Wiley and Sons, New York.

Tokimatsu, K. (1990). System compliance correction from pore pressure response in undrained triaxial tests. *Soils and Foundations*, 30(2):14–22.

Tokimatsu, K. and Nakamura, K. (1986). A liquefaction test without membrane penetration effects. *Soils and Foundations*, 26(4):127–138. https://doi.org/10.3208/sandf1972.26.4_127.

Towhata, I. (2008). *Geotechnical Earthquake Engineering*. Springer.

Vaid, Y., Fisher, J., Kuerbis, R., and Negussey, D. (1990). Particle gradation and liquefaction. *Journal of Geotechnical Engineering*, 116(4):698–703.

Vaid, Y. and Negussey, D. (1984). Relative density of pluviated sand samples. *Soils and Foundations*, 24(2):101–105. https://doi.org/10.3208/sandf1972.24.2_101.

Wichtmann, T. (2005). *Explicit accumulation model for non-cohesive soils under cyclic loading*. PhD thesis, Ruhr-University Bochum, Heft 38.

Wichtmann, T., Steller, K., Triantafyllidis, T., Back, M., and Dahmen, D. (2019). An experimental parametric study on the liquefaction resistance of sands in spreader dumps of lignite opencast mines. *Soil Dynamics and Earthquake Engineering*, 122:290–309. https://doi.org/10.1016/j.soildyn.2018.11.010.

Wolffersdorff, P.-A. v. (1996). A hypoplastic relation for granular materials with a predefined limit state surface. *Mechanics of Cohesive-Frictional Materials*, 1:251–271. https://doi.org/10.1002/(SICI)1099-1484(199607)1:3<251::AID-CFM13>3.0.CO;2-3.

Appendix A. Undrained cyclic tests

The tests were performed in a cyclic triaxial test device using samples of 10 cm diameter and 10 cm height otherwise samples of 15 cm diameter and 15 cm height. A scheme of the devices at IBF, KIT is shown in Fig. 9. The samples were prepared by moist tamping and tested in the water-saturated condition using a back pressure of $u = 500$ kPa. The effective lateral stress σ_3' was kept constant, while the cyclic loading was applied in the vertical direction, with an average value of effective axial stress $\sigma_1'^{\text{av}}$ and a stress amplitude σ_1^{ampl}. The cyclic loading was realized by means of a spindle gear system and a rate of 0.005 mm/min. Axial deformations were measured with a displacement transducer attached to the load piston, while volume changes were obtained from a burette system connected to the fully water-saturated pore space, using a differential pressure transducer. The specimen is considered completely liquefied according to the criterion (39). All tests are performend on Karlsruhe Sand, a clean medium sand with mean grain size $d_{50} = 0.54$ mm and a uniformity coefficient $C_u = d_{60}/d_{10} = 1.46$.

Appendix B. Formulas for k_{MP}

According to Nicholson et al. [1993], the volumetric strain ε^{MP} is a function of lateral compression from σ_{r0} to σ_r. It

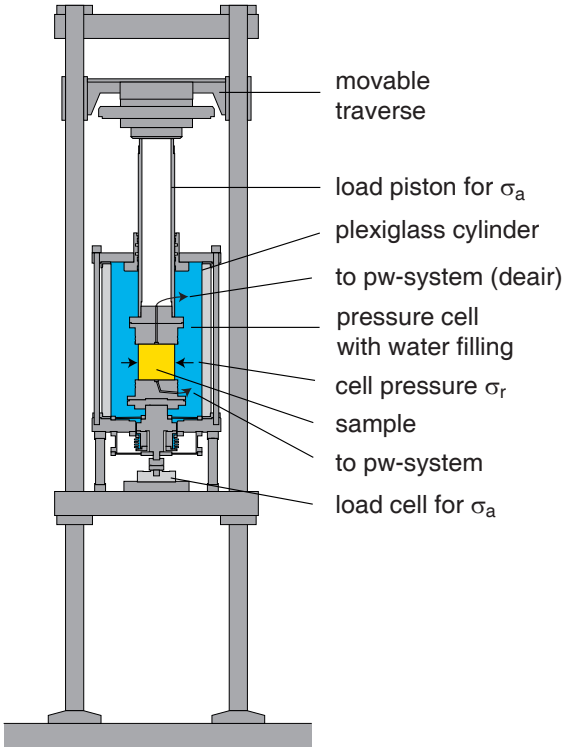

Figure 9. *Scheme of the cyclic triaxial tests used for this study at Institute for Soil and Rock mechanics, at the Karlsruhe Insitute for Technology*

can be estimated with the logarithmic compliance S^{MP} [cm],

$$\varepsilon_{\text{vol}}^{\text{MP}} = \frac{A_{\text{mem}}}{V} S^{\text{MP}} \ln \frac{\sigma_r}{\sigma_{r0}} \text{ or } \dot{\varepsilon}_{\text{vol}}^{\text{MP}} = \frac{A_{\text{mem}}}{V} S^{\text{MP}} \frac{\dot{\sigma}_r}{\sigma_r}, \quad (40)$$

where A_{mem}[cm^2] and V[cm^3] denote the area of the membrane and the sample volume, respectively. The previously used constants c_{MP} and k_{MP} should be upgraded accordingly to the functions of σ_r, i.e.

$$k_{MP}(p,q) = \frac{V\sigma_r}{AS^{\text{MP}}} \quad \text{with} \quad \sigma_r = p - q/3 \quad (41)$$

In order to determine S^{MP} experimentally, samples with different ratios A/V can be loaded identically isotropically. The deformation $\varepsilon_{\text{vol}}^{\text{MP}}$ increases proportionally with the ratio A/V and $\varepsilon_{\text{vol}}^{\text{MP}}$ can be estimated from the asymptotic value at $A/V \to \infty$.

The size of MP depends mainly on the grain size distribution curve. The number of pores, the grain shape, the structure of the grain skeleton and (surprisingly) the membrane strength or stiffness (if "usual" ratios of grain diameter to membrane strength are observed) are negligible. The following correlation between S^{MP} and grain diameter d_{20} was proposed in Nicholson et al. [1993], see Fig. 10.

$$S^{\text{MP}} \approx 0.0019 + 0.0095\, d_{20} - 0.0000157\, (d_{20})^2 \quad (42)$$

with units S^{MP} [cm] and d_{20} [mm].

An alternative formula

$$\varepsilon_{\text{vol}}^{MP} = \frac{1}{2} \frac{d_g}{D} \left(\frac{\sigma_r d_g}{E^M t^M} \right)^{1/3} \quad (43)$$

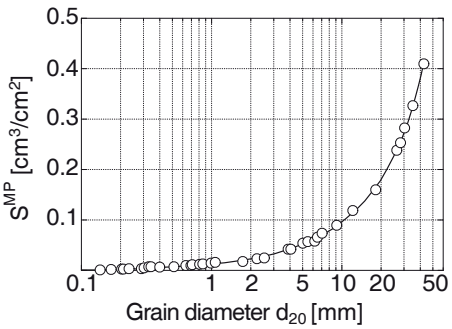

Figure 10. *Empirical formula (42) for S^{MP} as a function of the grain diameter d_{20}. Eq. (42) is not used in the example presented in Section 5.*

was proposed in Baldi and Nova [1984] with the grain diameter d_g[mm], diameter of the sample, D[mm], Young modulus of the membrane $E^M \approx 1.3 \cdot 10^3$ kPa, and the thickness of the membrane $t^M \approx 0,3$ mm. The corresponding rate

$$\dot{\varepsilon}_{\rm vol}^{MP} = C\sigma_r^{-2/3}\,\dot{\sigma}_r \quad \text{or} \quad k_{MP} = \frac{1}{C}\sigma_r^{2/3} \qquad (44)$$

$$\text{with} \quad C = \frac{1}{6}\frac{d_g}{D}\left(\frac{d_g}{E^M t^M}\right)^{1/3}$$

is in agreement with (2).

Appendix C. Mma scripts

Script 1. *Derivation of the stiffness for Section 3*

```
evs = ( p - q/3) /k ;    eqs = -evs/3;
e1 = p == K*(ev + evs) + Kpq (eq + eqs);
e2 = q == Kqp  (ev + evs)  + 3 G (eq + eqs);
solu = Solve[{e1, e2}, {p, q}] // FullSimplify
pp = p /. solu[[1]] ; qq = q  /. solu[[1]];

e1 = Ke == Coefficient[pp, ev]; e2 = Kepq == Coefficient[pp, eq];
e3 = Keqp == Coefficient[qq, ev]; e4 = Ge == Coefficient[qq, eq
     ]/3;
Solve[{e1, e2, e3, e4}, {K, G, Kpq, Kqp} ]
```

Script 2. *First derivation for Section 4.2*

```
e2 = 3 p == sa + 2 sr; e3 = q == sa - sr;
Solve[Eliminate[{e2, e3}, {sa}], sr];  dsr = dp - dq/3;
Solve[Eliminate[{dp,dq} == {{K, Kpq}, {0, 3 G}}.{-dsr/kMP, deq},
      deq+dsr/(3 kMP)], dp]
```

Script 3. *Second derivation for Section 4.2*

```
eq = Eliminate[{(G*K+ kMP Kpq)/(3G(K+kMP))==h,
                K/kMP== b,Kpq/(3*G)== h0},
                 {K,G,KMP}][[1]];
Solve[eq,h0]
```

Script 4. *Third derivation for Section 4.2*

```
stateU = {{100, 0}};  ASkempton = -0.1; ninc = 2000;
Do[ dq=0.5Cos[0.01*i];
    AppendTo[stateU, Last[stateU]+ {ASkempton*Abs[dq],dq}],
    {i,0,ninc}];
incrT = Transpose[  Drop[stateU, 1] -  Drop[stateU, -1] ];
hs =incrT[[1]] / incrT[[2]];
stateI = {{100, 0}};  beta = 0.2;
Do[dq = 0.5 Cos[0.01 i] ;
   h = hs[[i]]; h0 = h + beta (h - 1/3)  ;
   AppendTo[stateI, Last[stateI] + {  h0* dq , dq  }   ];
   , {i,1,ninc-1}];
ListPlot[{stateU,stateI}]
```

Mathematica script for the flow chart in Section

Script 5. *Main script for correction of undrained cyclic tests*

```
(* read the raw data *)
inn = OpenRead[  "data_150_20.dat" ];
nlines = 5000000;
nic = Array[0 &, nlines];
Do[ nic[[i]] = ReadLine[inn] ; iEnd = i;
    If[nic[[i]]=== EndOfFile, Print["final record=", i];
       Break[]];
 , {i,1,nlines}];
Close [inn] ;
nic = Take[nic, iEnd - 1 ];
Do[ If[ StringTake[ nic[[i]], 1] === "#", ,iEndComment = i;
       Break[]]
   ,{i, 1, 100} ] ;
nicPure = Drop[nic, iEndComment - 1];
nicTable = ( StringSplit[#] & /@ nicPure ) ;
{nelem, nitem} = nicTable // Dimensions;
Print["WAIT!"];
eStress = Array[0 &, nelem];
ProgressIndicator[Dynamic[ ie/nelem] ]
Do[ eStress[[ie ]]= Internal`StringToDouble[#]& /@ nicTable[[ie]]
  ,{ie, 1, nelem} ];

(* set the parameters for the  material stiffness *)
p =.;
thisSand= {e0 -> 0.74274, hB -> 2860030000, nB -> 0.21378,
           pZ -> 25, Z-> 2}  ;
(* for Bauer eq. e=e0 *Exp[-(3*p/hB)^nB ] with Osinov modif. *)

(* set the parameters for the  membrane *)
thisMembrane= {S ->  0.0039, AmV0 ->  0.27, dg ->  0.2, dP -> 100,
  EM -> 1550, tM -> 0.3, CBaldi -> (dg/dP)/6 *( dg/EM /tM)^(1/3)};
 (* valid for 50-100 kN, AmV0_150=0.27  AmV0_100=0.4; *)

(* Bulk modulus as a  function of eff. pressure *)
e = e0 *Exp[-(3*p/hB)^nB ] ;
dedp = -((3^nB*e*nB*(p/hB)^nB)/p);
depsvde = - 1/(1 + e); depsvdp =  depsvde * dedp // Simplify;
KB =  1/ depsvdp ;        (* bulk modulus  Bauer *)
K=  KB*(1-Exp[- p/pZ ])^(Z-nB);  (* multiplier Osinov *)


(* Perform the correction  *)
{s1, s3 , q, p, pcorr } = path[[1]];
pc = Array[0 &, nelem];  pc[[1]] = p;
ProgressIndicator[Dynamic[ ie/nelem] ]
Do[  {s1, s3 , q, p, pcorr } = path[[ie]];
   p = Max[p, 0.1];
   {ds1, ds3 , dq, dp, dpcorr } = path[[ie]] - path[[ie - 1]];
   kMP=  p ^(2/3) / CBaldi    //. thisMembrane;  (* Baldi *)
   kMP=(1/(S*AmV0)) *Max[s3,0.1]/. thisMembrane; (* Nicholson *)
   thisK = K /. thisSand;
   beta = thisK/kMP;
    pc[[ie]] = pc[[ie - 1]] + dp + beta*( dp - dq/3 ) ;
, {ie, 2, nelem}];

(*Paths meaured vs. corrected + shifted right by Dp=78 *)
ps = path[[All, 4]]; qs = path[[ All, 3  ]];
pcorrs = path[[All, 5]];
g1 = ListLinePlot[{Transpose[{ps, qs}],Transpose[{78+pc, qs}]},
                  PlotRange -> Full]
```

A MATLAB version of the above script is available from the authors.

Appendix D. Parameters for the MP correction procedure from Section 5

The presented correction of undrained cyclic tests requires the parameter S^{MP} of the membrane. After Nicholson et al. [1993], one could use the correlation of S^{MP} with d_{20}, cf. Eq. (42). Alternatively, one can evaluate S^{MP} directly from drained isotropic compression tests on cylindrical samples of different size (diameter = 2r = height), here 5, 10 and 15 cm. All samples were perfectly water-saturated under a constant back pressure u = 500 kPa. The sand and the membrane (thickness t_M = 0.3 mm, elastic modulus E_M = 1550 kPa) were identical as the ones in the undrained cyclic test, of course. The densities of all specimens were similar, D_{r0} = 39% - 42%, see Fig. 11a. All samples were subjected to identical isotropic, drained compression from p = 50 to 200 kPa. The volume changes were measured via the pore water system. The measured volumetric strain $\varepsilon^*_{\mathrm{vol}} = V_w/V_0$ was not identical for all samples. Additional volume V_w^{MP} due the MP was proportional to the surface A_{mem} of the membrane $2\pi r \cdot r$. The strain $\varepsilon_{\mathrm{vol}}^{\mathrm{MP}} = V_w^{\mathrm{MP}}/V$ with $V = \pi r^2 \cdot r$ must be therefore proportional to $1/r$. This explains why larger samples had smaller $\varepsilon^*_{\mathrm{vol}}$. The parameter S^{MP} [cm] was determined from the approximation of three measurements[12] of $\varepsilon^*_{\mathrm{vol}}$ by the Nicolson's formula

$$\varepsilon^*_{\mathrm{vol}} = \varepsilon_{\mathrm{vol}} + \frac{A_{\mathrm{mem}}}{V} S^{\mathrm{MP}} \ln \frac{\sigma_r}{\sigma_{r0}} \tag{45}$$

see Fig. 11a. For samples 5, 10 and 15 cm, the ratios were A_{mem}/V_0 were 0.8, 0.40 and 0.27 cm^{-1}, respectively, but $\ln(\sigma_r/\sigma_{r0}) = \ln 4$ was identical. Therefore, true deformation $\varepsilon_{\mathrm{vol}}$ is also assumed identical. The system of three independent equations (45) with two unknowns S^{MP} and $\varepsilon_{\mathrm{vol}}$ is overdetermined and gives the approximation $S^{MP} \approx 0.0039$cm, see Fig. 11a. Substituting this value into (41) for samples of size 15 cm one obtains roughly $k_{MP} \approx 1000p$.

The presented MP-correction requires the bulk stiffness $K(p)$ of soil skeleton in Eq. (37). During an undrained cyclic test, the effective pressure p decreases and hence the stiffness upon unloading is more appropriate than the one upon loading, Fig. 11 b). Using the approximation $e = e_0 \exp((-3p/h_B)^{n_B})$ after Bauer [1992], which corresponds to Eq. 37 the parameters e_0 = 0.742274, $h_B = 2.860 \cdot 10^9$ kPa and n_B = 0.21378 could be determined. For the modification of K at very low stress, the parameters after Osinov p_z = 50 kPa and ζ = 2 were used. The critical friction angle of Karlsruhe Sand is $\varphi = 33.1°$.

Manuscript received 17th January 2020, revised 25th May 2020 and 23rd September 2020, accepted 22nd September 2020.

[12] They correspond to diameters $2r$ = 5, 10 and 15 cm.

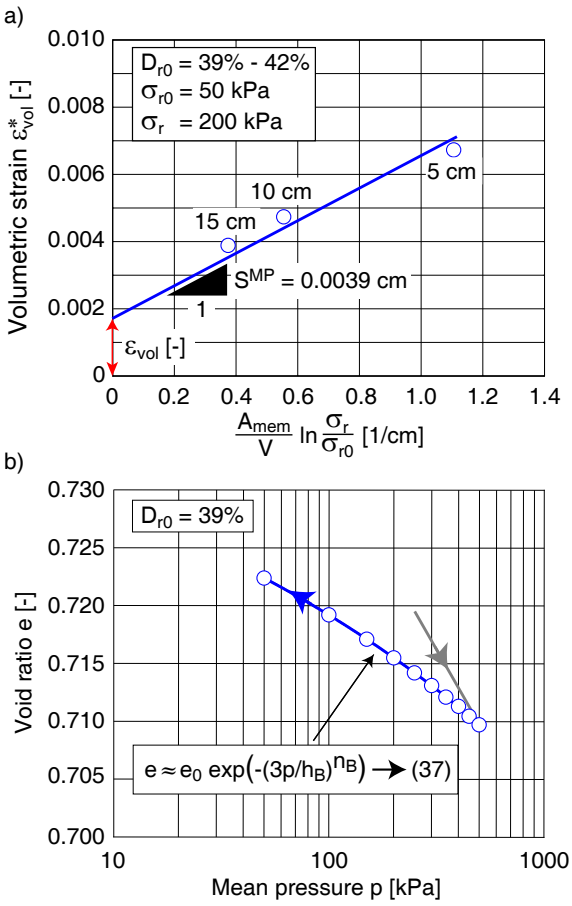

Figure 11. *a) Nicholson's membrane parameter S^{MP}. Volumetric strains $\varepsilon^*_{\mathrm{vol}}$ from samples of different size have been approximated by Eq. (45).*
b) Parameters for bulk modulus of skeleton K from drained triaxial tests with similar relative Density $D_{r0} \approx 40\%$. The parameters n_B and h_B were fitted to the unloading curve, and not to the first loading as required by Bauer [1992] for the constitutive description.